Molecular Biology of the Cell
Vol. 15, 5724–5732, December 2004

Direct Visualization of Microtubule Flux during Metaphase and Anaphase in Crane-Fly Spermatocytes

James R. LaFountain, Jr.,*† Christopher S. Cohan,‡ Alan J. Siegel,* and Douglas J. LaFountain*

Departments of *Biological Sciences and ‡Pathology and Anatomy, University at Buffalo, Buffalo, NY 14260

Submitted August 27, 2004; Accepted September 27, 2004
Monitoring Editor: J. Richard McIntosh

Microtubule flux in spindles of insect spermatocytes, long-used models for studies on chromosome behavior during meiosis, was revealed after iontophoretic microinjection of rhodamine-conjugated (rh)-tubulin and fluorescent speckle microscopy. In time-lapse movies of crane-fly spermtocytes, fluorescent speckles generated when rh-tubulin incorporated at microtubule plus ends moved poleward through each half-spindle and then were lost from microtubule minus ends at the spindle poles. The average poleward velocity of ~0.7 μm/min for speckles within kinetochore microtubules at metaphase increased during anaphase to ~0.9 μm/min. Segregating half-bivalents had an average poleward velocity of ~0.5 μm/min, about half that of speckles within shortening kinetochore fibers. When injected during anaphase, rh-tubulin was incorporated at kinetochores, and kinetochore fiber fluorescence spread poleward as anaphase progressed. The results show that tubulin subunits are added to the plus end of kinetochore microtubules and are removed from their minus ends at the poles, all while attached chromosomes move poleward during anaphase A. The results cannot be explained by a Pac-man model, in which 1) kinetochore-based, minus end-directed motors generate poleward forces for anaphase A and 2) kinetochore microtubules shorten at their plus ends. Rather, in these cells, kinetochore fiber shortening during anaphase A occurs exclusively at the minus ends of kinetochore microtubules.

INTRODUCTION

Successful segregation of chromosomes during either mitosis or meiosis depends upon the interaction between the kinetochores of chromosomes and the dynamic microtubules of the mitotic or meiotic spindle. There is evidence that microtubules attached to kinetochores (i.e., kinetochore microtubules) remain dynamic, even after their plus ends have attached to kinetochores. Using methods to introduce fluorescent markers at points along the length of kinetochore fibers (bundles of kinetochore microtubules), previous investigators have obtained clear evidence from different types of mitotic vertebrate cells (Mitchison, 1989; Mitchison and Salmon, 1992; Zhai *et al.*, 1995), from *Drosophila* embryos (Maddox *et al.*, 2002; Brust-Mascher and Scholey, 2002), and from *Xenopus* oocyte extracts (Sawin and Mitchison, 1991; Desai *et al.*, 1998; Maddox *et al.*, 2003) for microtubule flux, a steady poleward movement of kinetochore microtubules achieved through the balanced addition of tubulin subunits to microtubule plus ends at kinetochores and removal from minus ends at the spindle poles. Microtubule flux seen at metaphase then continues during anaphase A through the removal of subunits from the minus ends of kinetochore microtubules as chromosomes move poleward and kinetochore microtubules shorten (reviewed by Maddox *et al.*, 2003).

Article published online ahead of print. Mol. Biol. Cell 10.1091/mbc.E04–08–0750. Article and publication date are available at www.molbiolcell.org/cgi/doi/10.1091/mbc.E04–08–0750.

The online version of this article contains supplemental material at MBC Online (http://www.molbiolcell.org).

† Corresponding author. E-mail address: jrl@buffalo.edu.

In view of the persistence of flux-based depolymerization occurring at poles during anaphase, the theme emerging from those earlier studies is that microtubule flux definitely must play a role in chromosome segregation, and it may even dominate during anaphase A in some systems, namely *Drosophila* embryos (Maddox *et al.*, 2002; Brust-Mascher and Scholey, 2002) and *Xenopus* oocyte extract spindles (Desai *et al.*, 1998; Maddox *et al.*, 2003), based on comparisons of flux velocities with velocities of anaphase chromosomes. However, it is also clear that an additional locus (and in fact the major locus in cultured cells from vertebrates) of kinetochore microtubule shortening during anaphase A is the kinetochore (Rieder and Salmon, 1994). Thus, a mechanism based on a combination of microtubule flux and kinetochore-based depolymerization (the microtubule flux/Pac-man model) has gained general acceptance as an explanation for how these different systems achieve the segregation of chromosomes, with there being variability among the various systems as to which of the duo—microtubule flux or Pac-man—is emphasized. A kinetochore in the role of Pac-man is envisioned to embody the necessary minus end-directed motors and microtubule plus end "depolymerases" so that it could "chew" its way to the pole (Rieder and Salmon, 1998).

The universality of the Pac-man model as a required component of the mechanism underlying anaphase A has been questioned, based on evidence from a number of studies (for review, Pickett-Heaps and Forer, 2001), including recent findings from crane-fly spermatocytes in which acentric chromosome fragments lacking kinetochores move poleward at velocities similar to those of kinetochore-containing chromosomes (LaFountain *et al.*, 2001). That result suggested the "flux machine" model, by itself, might provide a sufficient explanation for anaphase A in those spermatocytes.

Crane-fly spermatocytes previously were used by Wilson *et al.* (1994) in an antibody staining study, which also provided evidence, albeit indirect, that a mechanism based solely on microtubule depolymerization at the spindle poles may be operative in those cells. Results from a recent study by Chen and Zhang (2004) using grasshopper spermatocytes suggest an anaphase Pac-man mechanism is not used in those cells either. One of the objectives of the work reported here was to directly test whether the microtubule flux/Pac-man model is operative during crane-fly meiosis.

Present findings are significant from two standpoints. Long recognized as ideal material for studies of chromosome movement during meiosis, insect spermatocytes have not figured prominently so far in studies that required microinjection, because of difficulties encountered when trying to inject them using standard pressure injection techniques. Progress toward overcoming this obstacle is being made: by others (Chen and Zhang, 2004), who have developed a high-pressure injection system, and in our laboratory, where we have determined conditions by which the iontophoretic microinjection of spermatocytes can be done routinely. In presenting our approach, we are expectant that it may open the way for similar studies on other types of cells that are not readily injected with standard pressure injection techniques.

More importantly, through our use of fluorescent speckle microscopy (Waterman-Storer *et al.*, 1998; Waterman-Storer and Salmon, 1998) we report the first direct observation of microtubule flux in crane-fly spermatocytes and present data concerning flux rates exhibited by kinetochore microtubules in relation to chromosome movements. Flux velocities during anaphase A were found to be significantly faster than chromosome velocities, indicating the addition of tubulin subunits to the plus ends of kinetochore microtubules as segregating chromosomes moved toward the pole. Those data are not in agreement with a Pac-man model. Instead, they show that kinetochore microtubules shorten during anaphase A in these meiotic cells exclusively at their minus ends.

MATERIALS AND METHODS

Spermatocyte Culture

For microinjections and subsequent fluorescent speckle microscopy (FSM), spermatocytes from the crane fly, *Nephrotoma suturalis*, were spread at the oil-glass interface of a well slide, which was made by sealing a coverglass over the circular hole cut in an aluminum plate that had the same dimensions as a glass microscope slide (Janicke and LaFountain, 1986). Only the highly flattened spermatocytes in such oil preparations were subjected to microinjection; rounded cells invariably rolled away from the injection pipette and therefore were useless. This report is based on data obtained from 63 microinjected cells.

Microinjections

Our attempts at pressure injection confirmed the fruitlessness of that approach to our material. In contrast, the iontophoretic approach is virtually 100% efficient, and we now use it routinely for FSM, as well as to inject other charged, nonpermeable compounds into crane-fly spermatocytes. For FSM of microtubules, rhodamine-conjugated (rh)-tubulin (Cytoskeleton, Denver, CO) diluted to 30 μM in 50 mM K glutamate, 0.5 mM KCl, pH 7.0 buffer (Waterman-Storer and Salmon, 1997) was loaded into the tip of a micropipette made in a Sutter model P-30 micropipette puller (Sutter Instruments, Novato, CA) using thin-walled, borosilicate glass (AM Systems, Everett, WA). The micropipette was held and positioned against the cell membrane using a hydraulic micromanipulator (Narashige Instruments) under visual control (40× or 100× objective). The solution in the micropipette contacted a silver wire that was connected to an intracellular amplifier (Getting Instruments, Iowa City, IA). A silver ground wire connected to the amplifier headstage was positioned nearby in contact with the testicular fluid bathing the cells under oil. To microinject, a brief oscillating voltage (pulse) was applied to the micropipette using the capacitance feedback control on the amplifier. The volume of rh-tubulin injected was a function of the duration of the current pulse (described in *Results*). To estimate the injected volume, carboxyfluorescein was injected into cells, and subsequent fluorescence intensity within cells was compared with fluorescence intensity of carboxyfluorescein in glass capillaries having the same thickness as cells. From those model data, we estimated the volume injected during a short 2-s pulse was ~500 femtoliters (1/100th of a typical spermatocyte volume), whereas a long 4-s pulse (or two 2-s pulses) yielded ~1/50th of a typical spermatocyte volume.

Fluorescent Speckle Microscopy

All microinjections and subsequent time-lapse FSM recordings were done on a Nikon inverted Diaphot 300 (Garden City, NY) equipped with a dry condenser (0.85 NA) for phase or differential interference contrast (DIC) imaging. FSM was done using a 100×/1.4 NA Plan Apochromat objective with mercury arc illumination, attenuated with a 1.0 neutral density filter and heat filter. Two-second, 16-bit images were captured with a cooled, back-illuminated CCD camera (Princeton Instruments, Princeton, NJ) controlled by IP lab software (Scanalytics, Fairfax, VA) after 4× projection. Computer-controlled shutters were placed in the transmitted and epi light paths to limit exposure. To obtain images from the same cell during both metaphase and anaphase, one image stack containing 24 or 48 frames was made over a duration of 6 min at metaphase, and then after the onset of anaphase, another 24 or 48 frames were made of anaphase using both DIC and fluorescence modes. Images in each mode were alternately collected, requiring manual switching of optical components in the illumination pathway between each exposure at intervals ranging from 7.5 to 30 s. That regimen was without effect on either specimen focus or frame registration in the images that were collected, as confirmed in a model experiment in which 0.2-μm diameter fluorescent beads (Fluoresbrite YG microspheres, 0.2 μm; Polysciences, Warrington, PA) were prepared as specimens and then recorded using the same time-lapse regimen used to record cells (our unpublished results).

Image Analysis

All image processing and analysis was done with IP Lab software (Scanalytics), and published images were prepared using Adobe Photoshop (San Jose, CA). To determine chromosome velocities during anaphase, measurements of partner kinetochore separation were made from DIC mode images using the IP Lab line measurement tool, and subsequently data were imported into Excel (Microsoft, Redmond, WA) for plotting. Data concerning spindle pole separation (anaphase B) were obtained likewise from DIC mode images using the line measurement tool to measure the distance separating the polar basal bodies located at the core of each centrosome. Analysis of speckle velocity was performed on fluorescence mode image stacks by manual tracking or by using a projection command supplied with IP lab software. Manual analysis was done only on speckles that remained visible or in focus for at least five consecutive time points (typically, a duration of 1 min or more). A script including the following steps was used to make projections: 1) the pixel value of each frame was scaled to the mean fluorescence intensity of the stack after background subtraction using the *3D Equalize* command, 2) the brightness and contrast of all frames in the stack were adjusted using the *Normalization* command, 3) the stack was rotated using the *Scale and Rotate* command so that the spindle was positioned vertically, 4) a region of interest (ROI) was positioned around a kinetochore fiber, 5) that ROI within every frame in the stack was duplicated to form a separate stack, which was converted to 8-bit data, and 6) the *3D Projector* command was used to create a projection stack in which the movement of speckles from one frame to the next was displayed as a function of time within the resultant 3-D projection. Projections are similar to the kymographs used to display time-dependent speckle movement in other studies (Waterman-Storer *et al.*, 1998). Statistics were done using Microsoft Excel and Fathom Dynamic Statistics (Key Curriculum Press, Emeryville, CA) software.

RESULTS

Primary spermtocytes of *N. suturalis* enter the reduction division of meiosis (meiosis I) with three autosomal bivalents and a small sex bivalent. The latter contains replicated X and Y chromosomes that disjoin precociously at prometaphase to yield two sex univalents. The behavior of univalents is unorthodox in that they display amphitelic orientation (vs. disyntelic for bivalents) during meiosis I, and they do not segregate poleward during anaphase A but lag at the spindle equator until telophase/cytokinesis when they move to opposite poles. Autosomal bivalents and the half-bivalents derived from them display orthodox behavior during anaphase A, and thus, they have been chosen as the subjects of the present study.

At metaphase (Figure 1), the spindle in a primary spermatocyte is large (typically 25–30 μm long from pole to pole by 15 μm wide at the equator in the highly flattened cells

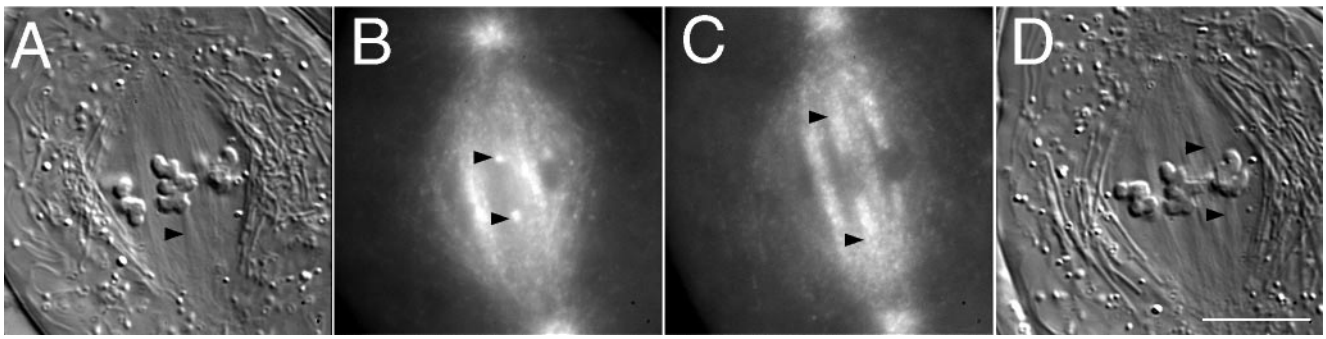

Figure 1. Spindle microtubules incorporate bovine rhodamine-tubulin. (A) DIC mode image of a crane-fly spermatocyte at metaphase made 45 s after a 4-s pulse (~1 picoliter) injection of 30 μM rh-tubulin. This optical section includes portions of all three bivalents and one of the kinetochore fibers attached to the middle bivalent is in sharp focus (arrowhead). (B and C) Wide-field fluorescence mode images of the cell in A, revealing fluorescence incorporation into kinetochore fibers initially at the kinetochores (arrowheads in B) and then spreading poleward with time (arrowheads in C). (B) 1 min after injection; (C) 10 min after injection. (D) Another DIC mode image made 13 min after injection illustrating a different optical section and additional kinetochore fibers (arrowheads) in sharp focus. Bar, 10 μm.

used here) and has a complex structure made up of hundreds of microtubules that occupy ~10% of the spindle mass. Kinetochore fibers containing densely bundled kinetochore microtubules are readily distinguished in DIC images (Figures 1, A and D; see also Figure 3, A and C) extending poleward from the bivalents and the univalents. There are five kinetochore fibers per half-spindle: three from each of the autosomes and two from the univalents. Earlier EM studies (LaFountain, 1974, 1976; Janicke and LaFountain, 1986; Scarcello *et al.*, 1986) have shown that each of the fibers extending from the paired sister kinetochores of bivalents is actually two closely apposed fibers that are resolved at the LM level only in favorable views (Figure 3, A and C; LaFountain and Oldenbourg, 2004). EM analysis revealed a range of 68–113 microtubules per sister kinetochore pair. Not all of those would be expected to be in a DIC optical *Z*-section (0.5 μm thick) of an in-focus kinetochore fiber as in Figure 1A. Nevertheless, such an optical *Z*-section would be expected to contain at least 30–50 kinetochore microtubules in a plane just distal from the kinetochore. A 1-μm-wide optical *Z*-section section (0.5 μm thick) of an adjacent region of the spindle either between kinetochore fibers or between a fiber and the sheath of mitochondria that surrounds the spindle should contain between 10 and 20 nonkinetochore microtubules. Earlier reports also include details concerning kinetochore structure at both the EM (Janicke and LaFountain, 1986) and LM levels (LaFountain *et al.*, 1998).

Rh-tubulin Incorporates into Spindle Microtubules and Reveals Microtubule Flux

After microinjection of rh-tubulin from bovine brain into primary spermatocytes at late prometa- or metaphase, spindle microtubules immediately became fluorescent, indicating the injected subunits incorporated into polymer without delay. The two centrosomes also became fluorescent. When 4-s iontophoretic pulses (see *Materials and Methods*) were used, the plus ends of kinetochore fibers initially displayed intense, fairly uniform fluorescence (Figure 1B). Kinetochore fiber fluorescence spread poleward with time (Figure 1C). In the cases of nonkinetochore microtubules after 4-s pulses and all microtubules after injection using a 2-s pulse (Figures 2A and 3B), fluorescence appeared at discrete sites—speckles—as a consequence of stochastic incorporation of rh-tubulin onto plus ends of nonfluorescent microtubules (Waterman-Storer *et al.*, 1998; Waterman-Storer and Salmon, 1998). A fluorescent speckle likely was generated from a concentration of rh-tubulin subunits, as opposed to fluorescence emanating from a single rh-tubulin subunit incorporated into just one microtubule (Waterman-Storer and Salmon, 1999). After using either 2- or 4-s pulses to inject rh-tubulin, playback of time-lapse image stacks of kinetochore fibers (Supplementary Videos 1, 2, and 3) revealed the steady unidirectional poleward movement of speckles within the microtubule-containing domains of the two half-spindles. Bidirectional movement of speckles was found in equatorial domains between aligned chromosomes where the two half-spindles overlap.

Using an algorithm described in *Materials and Methods*, we made 3-D projections similar to kymographs to illustrate the

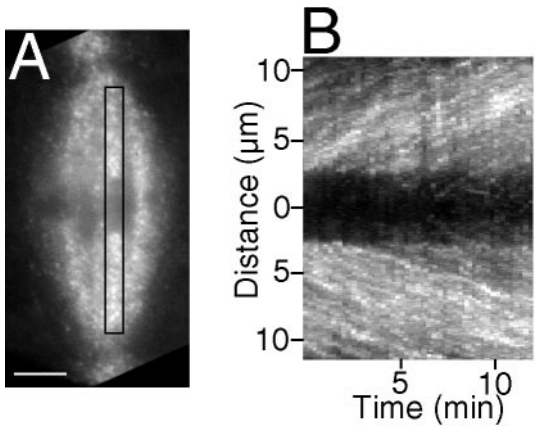

Figure 2. 3-D projection of speckle movements in kinetochore fibers. (A) The first frame of a 48-frame image stack (15-s intervals between frames) made of a spermatocyte at metaphase ~25 min after a 2-s pulse injection of rh-tubulin; a region of interest (ROI) is defined by the rectangle, and speckle movements within it appear in the 3-D projection. Bar, 5 μm. (B) 3-D projection prepared according to the algorithm detailed in *Materials and Methods* using the image stack of the spermatocyte in A. Poleward movement of speckles appears as linear tracks in projections, and the slopes of the tracks are their velocities. Ordinate: distance in μm; abscissa: time in minutes. This projection contains two arrays of tracks: one array containing speckles that move up within the kinetochore fiber directed to the upper pole in A, and the other array moving down within the partner's fiber, which is directed to the lower pole.

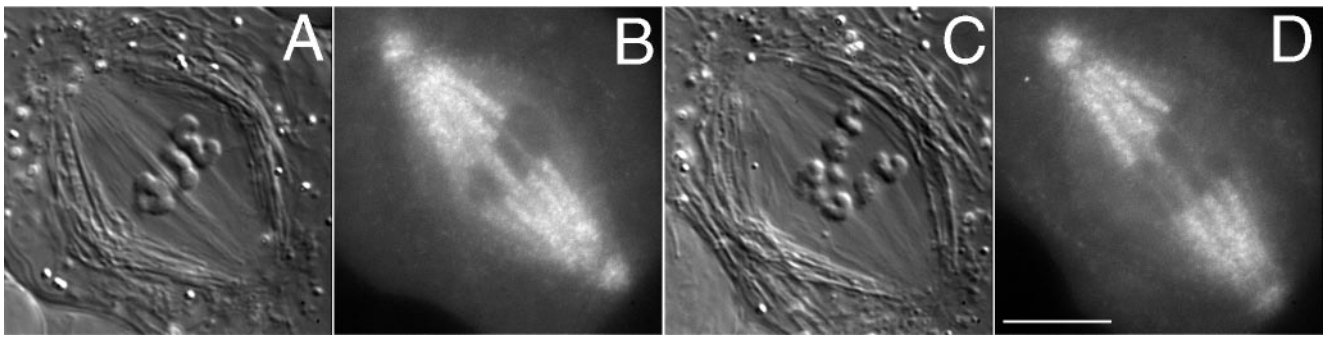

Figure 3. Alternate DIC-fluorescence mode images of metaphase and anaphase in the same cell. (A) DIC mode image of a spermatocyte at metaphase made ~25 min after a 2-s pulse injection of rh-tubulin. (B) In fluorescence mode, kinetochore fibers imaged with DIC in A appear speckled. (C and D) The same cell as in A and B undergoing anaphase A, during which kinetochore fibers shorten as autosomal half-bivalents segregate poleward. The two small sex univalents lag at the equator during anaphase A. Bar, 10 μm.

movement of speckles within kinetochore fibers as linear tracks (Figure 2B), the slopes of which were quantified to give the velocities of speckles as they moved from one frame to the next within an image stack. Based on slopes of 106 speckle tracks made from 34 kinetochore fibers in 9 spermatocytes at metaphase I, the average poleward speckle velocity was 0.7 ± 0.3 μm/min (Table 1). Manual tracking of speckles generated similar results with an average velocity for kinetochore fiber speckles of 0.6 ± 0.2 μm/min (Table 1; Figure 4B). Some of the kinetochore fiber speckles that were tracked manually emerged from the kinetochore regions of bivalents, providing confirmation that they were indeed kinetochore microtubule speckles. With all other speckles that were categorized as kinetochore microtubule speckles during manual tracking or in 3-D projections, the criterion used in identifying them was that they appeared to be part of a kinetochore fiber as detected with DIC (e.g., Figure 1, A-B and C-D and Figure 3, A-B and C-D). The possibility exists that some of the speckles identified as being kinetochore microtubule speckles were in fact nonkinetochore speckles, owing to the high density of microtubules in these spindles. However, based on velocity considerations (next paragraph), the relatively slower velocities of the majority of kinetochore microtubules that were analyzed suggest they were in fact correctly identified.

In regard to nonkinetochore microtubules in metaphase spindles, manual tracking in regions containing only them (i.e., between kinetochore fibers, between bivalents, and peripheral to both bivalents and their kinetochore fibers) generated an average speckle velocity of 0.8 ± 0.4 μm/min (Table 1), significantly faster than velocities of kinetochore microtubule speckles.

Poleward Microtubule Flux Persists during Anaphase A

On entering anaphase A, the poleward movement of speckles persisted, as shown in the movies we made of anaphase cells (Figure 3D; Supplementary Videos 4, 5, and 6). To quantify anaphase flux, we used the same approaches applied to metaphase cells: 3-D projections and manual tracking. For such analysis, only the first two-thirds of anaphase (during which kinetochore fibers shortened from ~10 to 3 μm) was useful. Toward the completion of anaphase, tilting relative to the plane of focus or dense packing of microtubules in the short remaining half-spindle precluded meaningful analysis. In addition, fluorescent signals diminished with time, and that resulted in unfavorable signal-to-noise ratios in late anaphase images that followed meta- and early anaphase images.

Nevertheless, we were able to make 3-D projections of kinetochore fiber speckles in 15 early to midanaphase cells

Table 1. Summary of speckle velocity and chromosome velocity data from cells injected at late prometa- or metaphase

Stage analyzed	Method of analysis	Kinetochore microtubule, (kMT) speckles	Nonkinetochore microtubule, (nkMT) speckles	Half-bivalent chromosomes
Metaphase	Projections	0.7 ± 0.3 μm/min (n = 106)		
	Manual tracking	0.6 ± 0.2 μm/min (n = 43)	0.8 ± 0.4 μm/min (n = 36)	
Anaphase	Projections	0.9 ± 0.2 μm/min (n = 213)		
	Manual tracking	0.9 ± 0.2 μm/min (n = 31)	0.9 ± 0.3 μm/min (n = 24)	0.5 ± 0.1 μm/min (n = 25)
Anaphase half-bivalent velocity in uninjected control cells				0.4 ± 0.1 μm/min (n = 28)

Student's *t* test: kMT anaphase projections vs. half-bivalent chromosomes: $p < 0.0001$; kMT anaphase projections vs. kMT metaphase projections: $p < 0.0001$; kMT anaphase manual vs. kMT metaphase manual: $p < 0.0001$; kMT metaphase manual vs. nkMT metaphase manual: $p = 0.0015$; kMT anaphase manual vs. nkMT metaphase manual: $p = 0.19$; nkMT metaphase manual vs. nkMT anaphase manual: $p = 0.22$; kMT anaphase manual vs. nkMT anaphase manual: $p = 1.0$

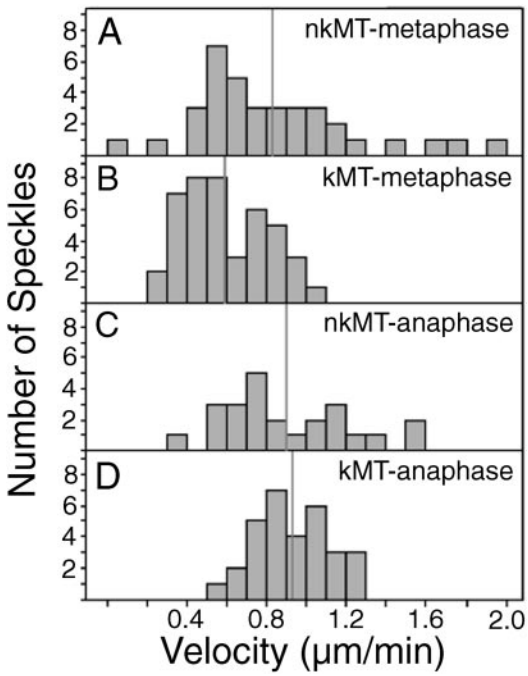

Figure 4. Summary of data obtained from manual tracking of speckles in metaphase and anaphase spindles. Histograms of speckle velocities exhibited by (A) nonkinetochore microtubules in metaphase spindles, (B) kinetochore microtubules in metaphase spindles, (C) nonkinetochore microtubules in anaphase spindles, and (D) kinetochore microtubules in anaphase spindles. Mean velocities are indicated with vertical gray lines.

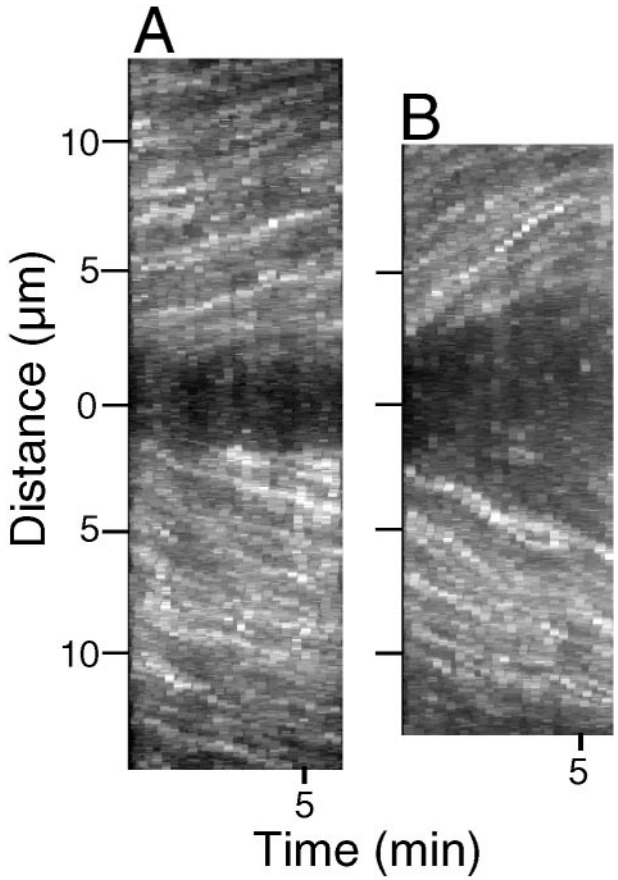

Figure 5. 3-D projections made using the same kinetochore fibers at metaphase and anaphase. (A) 3-D projection made using a 24-frame image stack (15-s intervals between frames) of a spermatocyte at metaphase ~40 min after a 2-s pulse injection of rh-tubulin. (B) 3-D projection of the same pair of kinetochore fibers projected in A using a 24-frame image stack made during anaphase A, when flux rates within kinetochore fibers are faster than at metaphase; slopes of speckle tracks in the projections of anaphase fibers (B) are steeper than tracks at metaphase (A).

and found an average velocity of 0.9 ± 0.2 μm/min (Table 1), significantly ($p < 0.0001$) greater than at metaphase (Table 1). Such differences are illustrated in the metaphase and anaphase projections made from the same fibers in one of the cells (Figure 5, A and B).

Manual tracking was used to make direct comparisons between anaphase and metaphase data from the nine cells for which we had movies of both meta- and anaphase A. That analysis yielded similar data: 0.9 ± 0.2 μm/min (Table 1; Figure 4D). Many of those manually tracked speckles appeared to emerge from kinetochores as anaphase progressed, confirming their identity as kinetochore microtubule speckles.

In regard to nonkinetochore microtubules during anaphase, the average velocity of their speckles was 0.9 ± 0.3 μm/min (Table 1; Figure 4C), similar to that for kinetochore microtubules during anaphase (Table 1; Figure 4C) and nonkinetochore microtubules during metaphase (Table 1; Figure 4A).

Speckles Move Poleward Faster than Segregating Chromosomes

Usually during anaphase A in crane-fly spermatocytes, disjoined half-bivalent chromosomes move poleward in a processive manner (Figure 6) with a velocity of ~0.5 μm/min (LaFountain *et al.*, 2001). In microinjected cells having speckled microtubules, the poleward velocity of speckles was nearly double the velocity of chromosomes (Table 1). During playback of time-lapse image stacks made during anaphase (Supplementary Videos 5 and 6), kinetochores appeared to be "spitting" speckles into the kinetochore fiber (as with a "reverse Pac-man" mechanism; Maddox *et al.*, 2003; see *Discussion*) as they moved poleward. We found no evidence for kinetochores overtaking speckles (as with a Pac-man mechanism), nor did we find any evidence for kinetochores moving at the same velocity as speckles (as if "parked" on kinetochore fiber plus ends). Using DIC image stacks (see *Materials and Methods*) of the same spermatocytes from which we obtained anaphase speckle velocity data above, we measured chromosome velocities and found (consistent with the published data) that the average poleward velocity of half-bivalents in injected cells was 0.5 ± 0.1 μm/min, significantly slower ($p < 0.0001$, Table 1) than the average kinetochore microtubule speckle velocity during anaphase within those cells (0.9 ± 0.2 μm/min).

To ensure the accuracy of the chromosome velocity measurements, anaphase B spindle elongation was assessed during anaphase A. Among the 10 anaphase cells in which spindle lengths were recorded at the onset and at the completion of anaphase A, the average increase in spindle length was 7 ± 3%, or an average length increase of ~2 μm. If spread over the duration of anaphase A (20 min), the anaphase B component during anaphase A amounts to ~0.1 μm/min, a factor that would not substantially influence the velocities of either microtubule speckles or the half-bivalents

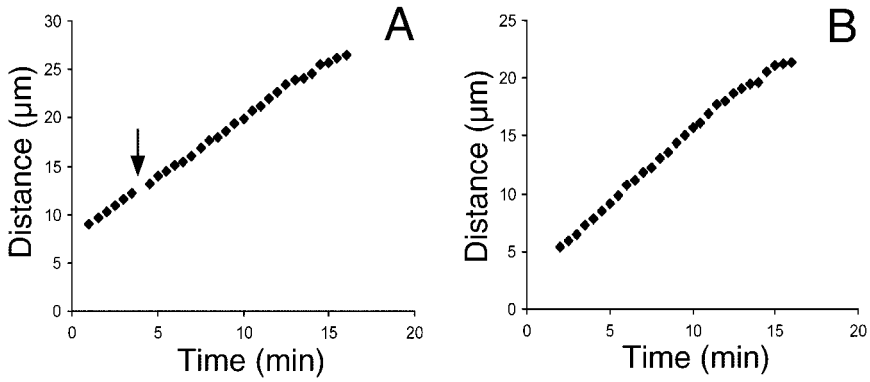

Figure 6. Distance vs. time plots of spatial separation of half-bivalent kinetochores during anaphase A yield linear velocity profiles. (A) A plot for partner half-bivalents in a spermatocyte that was injected with ~500 fl of 30 μM rh-tubulin during anaphase (arrow indicates the time of injection). (B) A similar plot of velocity of chromosome separation for a pair of half-bivalents in a control (not injected) cell.

attached to them. In fact, if anaphase B were contributing to chromosome separation, subunit addition at kinetochores during anaphase would need to be even more substantial to account for the observed chromosome velocity.

Injection of rh-tubulin during Anaphase Reveals Tubulin Subunit Addition at Kinetochores

Because it takes ~20 min to complete anaphase A in spermatocytes, there was sufficient time after the onset of anaphase to inject rh-tubulin into a spermatocyte undergoing anaphase and then assess whether subunits incorporated into shortening kinetochore fibers. When an injection was performed using a 4-s pulse, rh-tubulin fluorescence appeared initially at kinetochores and spread poleward as anaphase progressed, all while the fiber actually shortened at the pole (Figure 7, C and D; Supplementary Video 7). Incorporation of fluorescence into kinetochore fibers was observed regardless of whether injection was performed during early or mid-to-late anaphase A. The shortest kinetochore fiber into which we observed rh-tubulin incorporate was only 3 μm long. We did not attempt this operation on cells having fibers shorter than 3 μm.

When we used a 2-s pulse, rapid speckling of kinetochore and nonkinetochore microtubules was observed, and poleward movement of speckles was readily apparent. Analysis using the projection algorithm revealed an average poleward velocity of kinetochore speckles of 0.9 ± 0.4 μm/min (n = 30). The average poleward velocity of half-bivalents in those anaphase-injected cells was 0.5 ± 0.2 μm/min (n = 25).

Regardless of whether 2- or 4-s pulses were used for injection during anaphase, neither had any detectable adverse effect on the course of anaphase. Because the volume of rh-tubulin solution that was injected was so small relative to the volume of the cell, the appearance of an injected cell immediately after the operation was almost indistinguishable from that before injection (Figures 7, A and B). Poleward movement of half-bivalents after injection exhibited linear velocity profiles (Figure 6A), similar to that normally seen in control cells (Figure 6B). Chromosomes did not "back away" from the pole upon incorporation of rh-tubulin during anaphase as was reported by Shelden and Wadsworth (1992) using PtK_1 cells.

DISCUSSION

Microtubules translocate poleward in spindles of crane-fly primary spermatocytes with flux rates between ~0.6 and 0.9 μm/min, slower than the fast flux rates of ~2 μm/min found in *Xenopus* oocyte extract spindles (Sawin and Mitchison, 1991; Desai *et al.*, 1998; Maddox *et al.*, 2003) and 2–5 μm/min in *Drosophila* embryo spindles (Brust-Mascher and Scholey, 2002; Maddox *et al.*, 2002) but somewhat faster than the rate of ~0.5 μm/min in spindles of cultured vertebrate cells (Mitchison and Salmon, 1992; Zhai *et al.*, 1995). Those previous data suggested a correlation between flux rate of

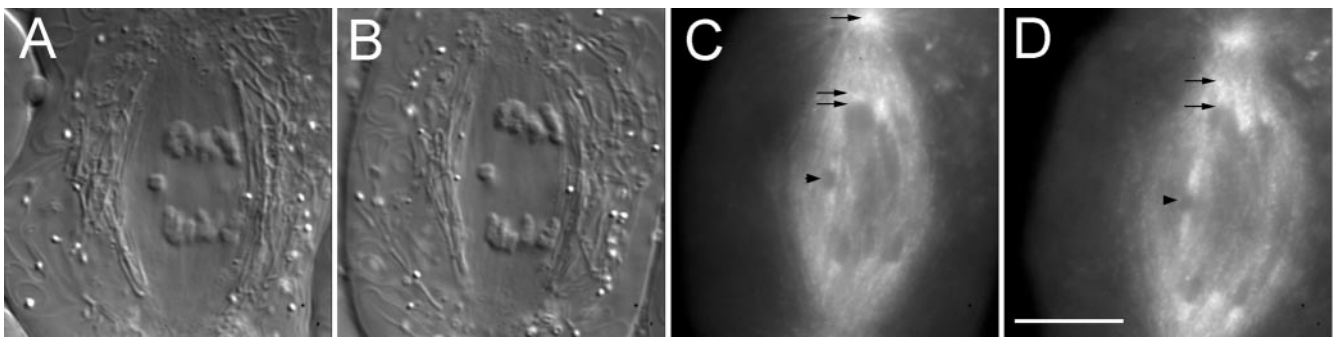

Figure 7. Kinetochore microtubules incorporate rh-tubulin at plus ends after a 4-s pulse injection during anaphase. (A) DIC image of a spermatocyte 1 min. before injection. (B) DIC image 50 s after a long pulse injection. (C and D) Selected frames from a wide-field fluorescence mode image stack made of the cell in A and B. (C) Two minutes after injection; rh-tubulin incorporates at kinetochores, one of which is located (lower arrow), causing the kinetochore-proximal portion of the kinetochore fiber to appear heavily labeled (middle arrow); upper arrow locates the centrosome. (D) Six minutes after injection, fluorescence of kinetochore fibers has spread poleward (upper arrow) from the kinetochore (lower arrow) while the distance between the kinetochore and centrosome has decreased, compared with C. Fluorescence of kinetochore fibers attached to sex univalents (arrowheads in C and D) also has spread poleward; compared with C. Bar, 10 μm.

spindle microtubules and the behavior exhibited by metaphase kinetochores attached to them. In vertebrate mitosis, where flux rates are slow, metaphase kinetochores exhibit oscillatory movement about the equator. In systems having fast flux rates, such oscillations are not observed. Bivalent kinetochores in crane-fly spermatocytes do not oscillate, and thus fast flux rates are expected. The fastest flux rates within nonkinetochore microtubules at metaphase (1.6–2.0 μm/min; Figure 4A) approached rates in *Xenopus* and *Drosophila* kinetochore microtubules. However, the average flux rates in spermatocytes, and in particular, the average of 0.6 μm/min for kinetochore fibers at metaphase, are closer in magnitude to slow rates of vertebrate mitosis than to fast flux rates reported for spindles in *Xenopus* extracts and *Drosophila* embryos. Thus, based on data from crane-fly spermtocytes, it is not clear whether a general correlation between flux rate and prometaphase/metaphase kinetochore behavior actually can be made. A clearer picture should emerge as fluorescent speckle microscopy is applied to other types of cells, possibly using the iontophoretic microinjection approach described here.

Our findings are in accord with results also obtained from crane-fly spermatocytes by Forer (1965, 1966), who used a UV microbeam to produce a localized area of reduced birefringence (ARB) on kinetochore fibers and then followed the subsequent poleward movement during both meta- and anaphase with polarized light microscopy. Although we still do not fully understand the structural composition of an ARB or how ARB integrity is maintained as it moves poleward, our data confirm the interpretation made from those early studies (reviewed by Forer and Wilson, 1994) that microtubule polymer on either side of the ARB is translocated poleward.

During at least the first two-thirds of anaphase A (the portion of anaphase analyzed here), the flux rate in spermatocytes is twice that of the segregating half-bivalents. Our direct visualization of microtubule flux in crane-fly spermatocytes has revealed that anaphase A proceeds according to the scheme in Figure 8. Kinetochore fiber shortening takes place exclusively at the polar minus ends of kinetochore fibers, while subunits are added at plus ends of kinetochore fibers as anaphase proceeds. We found no evidence for a Pac-man mechanism or for kinetochore bistability (alternation between Pac-man and reverse Pac-man) found by Maddox *et al.* (2003) in *Xenopus* oocyte extracts. Instead, kinetochores exhibited a reverse Pac-man mechanism through the duration of anaphase A that was analyzed. Such a continuous reverse Pac-man mechanism was predicted in a model for anaphase proposed by Chen and Zhang (2004), based on their work on grasshopper spermatocytes. Forer and Wilson (1994) also raised the possibility that such a mechanism could explain some of their results after UV microbeam irradiation of kinetochore fibers during anaphase.

A "short burst" of kinetochore-based depolymerization at the onset of anaphase in crane-fly spermatocytes was suggested from the work of Wilson *et al.* (1994), but we found no evidence for that. In the cells we recorded passing through the metaphase-anaphase transition, no discontinuity in movement of speckles away from kinetochores was noticed at the start of anaphase.

An additional noteworthy point is that microtubule flux within each half-spindle at rates in excess of chromosome velocities provides a ready explanation for chromosome arm behavior observed in crane-fly spermatocytes during anaphase (Adames and Forer, 1996; LaFountain *et al.*, 2001). As achiasmic arms associate with the microtubule lattice of each half-spindle, the "flux field" directs arms poleward and causes them to move ahead of kinetochores during anaphase A.

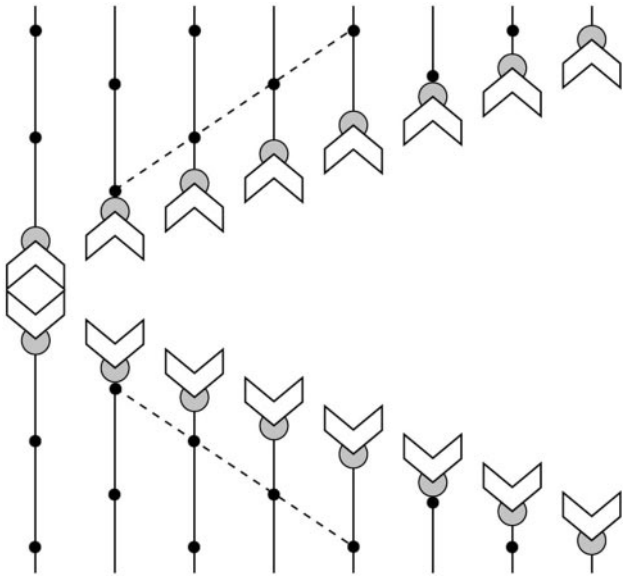

Figure 8. Scheme for anaphase A in crane-fly spermatocytes. Half-bivalents (chevrons) separate and segregate to opposite poles with processive, essentially linear trajectories. Kinetochore fibers (lines) shorten exclusively at the poles (top and bottom of diagram). Shortening does not occur at kinetochores (partial circle). Poleward flux is revealed by fluorescent speckles (dots), which move poleward during anaphase A with velocities (dashed lines) that are greater than the velocities of segregating half-bivalents. Rh-tubulin subunits are added at plus end of kinetochore microtubules at a rate that is slower than the rate of subunit removal at the spindle poles.

Polymerization at plus ends of kinetochore microtubules and deploymerization at minus ends during anaphase is a continuation of metaphase flux, in which the tubulin on-rate at kinetochore microtubule plus ends equals the tubulin off-rate at their minus ends. Speckle velocity data indicate that the flux rate of kinetochore microtubules during anaphase is ~30–50% faster than during metaphase. To accomplish that, the anaphase tubulin off-rate at kinetochore microtubule minus ends must also be 30–50% faster during anaphase (from Table 1, using projection data: $0.9 - 0.7/0.7$; using manual tracking data: $0.9 - 0.6/0.6$). It is not clear to us how such up-regulation of kinetochore microtubules is achieved. To speculate, perhaps the activities of minus-end "depolymerases" increase. In mitotic cells from vertebrates, a change in the flux rate at the metaphase-anaphase transition is just the opposite, decreasing at anaphase to about half the metaphase rate (Zhai *et al.*, 1995).

At the plus ends of kinetochore microtubules, the tubulin on-rate during anaphase must be ~30–40% slower than that at metaphase in order for chromosomes to move poleward with velocities of 0.5 μm/min (from Table 1, using projection data: $[0.7 - (0.9 - 0.5)]/0.7$; using manual tracking data: $[0.6 - (0.9 - 0.5)]/0.6$). Down-regulation of polymerization at kinetochores during anaphase occurs in the Pac-man model, such that plus-end polymerization ceases at anaphase onset as plus-end depolymerization is activated. Cessation of tubulin addition to kinetochore microtubule plus ends is also an integral feature of a model for anaphase A in which kinetochores are parked on the plus ends of fluxing kinetochore microtubules (see Maddox *et al.*, 2003, Figure 1B). In the latter, poleward motion of chromosomes would

proceed with a velocity equal to that of the microtubule flux rate, a mechanism thought to be operative in *Xenopus* extract spindles (Desai *et al.*, 1998) but recently shown to be Pac-man dependent (Maddox *et al.*, 2003). In the final minutes of anaphase A in newt lung cells, kinetochores park on kinetochore microtubules and are transported poleward exclusively by microtubule flux (Mitchison and Salmon, 1992).

Here we show that in crane-fly spermatocytes, kinetochores neither chew their way poleward nor are they parked on the plus ends of fluxing microtubules. Thus, in the case of these meiotic cells, an entirely new mechanism for anaphase A has been revealed, at least for the initial two-thirds of anaphase A. Half-bivalents are capable of moving poleward, even though reverse Pac-man is operative, because the rate of subunit removal at the spindle poles is greater than the rate of subunit addition at kinetochores.

The two "polymerization states" of kinetochores—one at metaphase and the other during anaphase—described here correspond to two states modeled by Maddox *et al.*, (2003), based on data from spindles in *Xenopus* oocyte extracts. Applying those ideas to spermatocytes, bivalent kinetochores would be in a "metaphase polymerization state" when they are motionless and subject to resistive tension (Figure 4A in Maddox *et al.*, 2003). The cause of such tension may be friction produced between kinetochore binding sites and translocating microtubules. The stretch and separation between sister kinetochores in mitotic systems provides evidence for such tension at metaphase (Waters *et al.*, 1996). In regard to meiotic systems, bivalents stabilized at the spindle equator have long been thought to be subject to bipolar tension (Nicklas, 1997). Friction between kinetochores and microtubules also may contribute to observed slower flux rates of kinetochore microtubules vs. nonkinetochore microtubules at metaphase.

In our "anaphase polymerization state," a kinetochore moves with a poleward velocity equal to the flux rate minus the plus-end polymerization rate. This state (reverse Pac-man) is also proposed by Maddox *et al.* (2003) to be a resistive state (their Figure 4B), in which kinetochores are responding to applied force, presumably through the imposition of tension of lesser magnitude than that at metaphase. With the anaphase polymerization state in spermatocytes, however, the reverse Pac-man mechanism is sustained, in contrast to the intermittent activation of this state observed in *Xenopus* extracts.

Segregating partner half-bivalents in crane-fly spermatocytes are connected by elastic tethers (LaFountain *et al.*, 2002a). During early to midanaphase A, tethers resist the poleward forces applied through kinetochores, as revealed through back-stretched arms of separated partners. When such arms are cut off with a laser, they move backward and can actually make contact with the telomere of their partner in the opposite half-spindle. We propose the resistance offered by tethers is insufficient to maintain the metaphase polymerization state but sufficient to support the sustained reverse Pac-man activity that is characteristic of crane-fly anaphase.

Our study of tethers revealed that the resistive forces imposed by them appear to diminish as anaphase progresses. Thus, in later anaphase, there may no longer be sufficient resistance to maintain the sustained reverse Pac-man activity of anaphase kinetochores. Because of technical difficulties in analyzing late anaphase, we cannot rule out the possibility that anaphase A in spermatocytes might also include a third state that appears during the final few minutes as chromosomes approach the poles. Maybe during that time, a depolymerization (Pac-man) mechanism is activated, or chromosomes park on kinetochore microtubules. Precedent for a change in the mechanism operating during late anaphase comes from work on vertebrate mitosis where late anaphase includes a slow-down in flux rate and cessation of Pac-man activity such that kinetochores become parked on microtubule plus ends (Mitchison and Salmon, 1992).

CONCLUSION

We conclude that motive forces for anaphase A in crane-fly spermatocytes are transmitted to chromosomes through kinetochores, rather than being generated by kinetochores.

The two half spindles in crane-fly spermatocytes have been characterized as being "flux machines" capable of translocating kinetochores, acentric chromosome fragments (LaFountain *et al.*, 2001) or sniglets (ribbons or globules that form upon laser microbeam denaturation; see LaFountain *et al.*, 2002a, 2002b) poleward at velocities similar to chromosomes. In that model, kinetochore fibers play the roles of traction fibers that are translocated poleward by any of a number of motor molecules, including plus end-directed motors that pull on the minus ends of kinetochore microtubules from the spindle poles (Chen and Zhang, 2004), plus end–directed motors within the spindle matrix that act along the lengths of kinetochore microtubules (Kapoor and Mitchison, 2001; reviewed by Kapoor and Compton, 2002), or an actin/myosin system (Silverman-Gavrila and Forer, 2000) deployed to translocate spindle microtubules poleward.

Although there is a strong tendency to view microtubule flux with a bias in terms of the action of molecular motors, it is possible that flux is instead a consequence of an intrinsic treadmilling property of spindle microtubules. There is now clear evidence for treadmilling in vivo, at rates of ~4 μm/min (Rodionov and Borisy, 1997), much faster than the very slow treadmilling rates (0.7 μm/h) reported in vitro (Margolis and Wilson, 1981). The concept of force generation simply through the assembly and disassembly of polymers is long-standing (Inoué and Sato, 1967), and a number of in vitro experiments have shown that depolymerizing microtubules can generate a pulling force and do work (for review, see Inoué and Salmon, 1995). What we need is a direct test of this model in living cells.

ACKNOWLEDGMENTS

We thank Jim Stamos for help with the figures and Marie Janicke for critical reading of the manuscript. This work was supported by grant MCB-0235934 to J.R.L. and IBN-0082793 to C.S.C. from the National Science Foundation.

REFERENCES

Adames, K.A., and Forer, A. (1996). Evidence for poleward forces on chromosome arms during anaphase. Cell Motil. Cytoskelet. *34*, 13–25.

Brust-Mascher, I., and Scholey, J.M. (2002). Microtubule flux and sliding in mitotic spindles of *Drosophila* embryos. Mol. Biol. Cell *13*, 3967–3975.

Chen, W., and Zhang, D. (2004). Kinetochore fibre dynamics outside the context of the spindle during anaphase. Nat. Cell Biol. *6*, 227–231.

Desai, A., Maddox, P.S., Mitchison, T.J., and Salmon, E.D. (1998). Anaphase A chromosome movement and poleward spindle microtubule flux occur at similar rates in *Xenopus* extract spindles. J. Cell Biol. *141*, 703–713.

Forer, A. (1965). Local reduction of spindle fiber birefringence in living *Nephrotoma suturalis* (Loew) spermatocytes induced by ultraviolet microbeam irradiation. J. Cell Biol. *25*, 95–117.

Forer, A. (1966). Characterization of the mitotic traction system, and evidence that birefringent spindle fibers neither produce not transmit force for chromosome movement. Chromosoma *19*, 44–98.

Forer, A., and Wilson, P.J. (1994). A model for chromosome movement during mitosis. Protoplasma *179*, 95–105.

Inoué, S., and Salmon, E.D. (1995). Force generation by microtubule assembly/disassembly in mitosis and related movements. Mol. Biol. Cell *6*, 1619–1640.

Inoué, S., and Sato, H. (1967). Cell motility by labile association of molecules: the nature of mitotic spindle fibers and their role in chromosome movement. J. Gen. Physiol. *50*, 259–292.

Janicke, M.A., and LaFountain, J.R., Jr. (1986). Bivalent orientation and behavior in crane-fly spermatocytes recovering from cold exposure. Cell Motil. Cytoskelet. *6*, 492–501.

Kapoor, T.M., and Compton, D.A. (2002). Searching for the middle ground: mechanisms of chromosome alignment during mitosis. J. Cell Biol. *157*, 551–556.

Kapoor, T.M., and Mitchison, T.J. (2001). Eg5 is static in bipolar spindles relative to tubulin: evidence for a static spindle matrix. J. Cell Biol. *154*, 1125–1133.

LaFountain, J.R., Jr. (1974). Birefringence and fine structure of spindles in spermatocytes of *Nephrotoma suturalis* at metaphase of first meiotic division. J. Ultrastruct. Res. *46*, 268–278.

LaFountain, J.R., Jr. (1976). Birefringence and ultrastructure of spindles in primary spermatocytes of *Nephrotoma suturalis* during anaphase. J. Ultrastruct. Res. *54*, 333–346.

LaFountain, J.R., Jr., and Oldenbourg, R. (2004). Maloriented bivalents have metaphase positions at the spindle equator with more kinetochore microtubules to one pole than to the other. Mol. Biol. Cell (*in press*).

LaFountain, J.R., Jr., Hard, R., and Siegel, A.J. (1998). Visualization of kinetochores and analysis of their refractility in crane-fly spermatocytes after aldehyde fixation. Cell Motil. Cytoskelet. *40*, 147–159.

LaFountain, J.R., Jr., Oldenbourg, R., Cole, R.W., and Rieder, C.L. (2001). Microtubule flux mediates poleward motion of acentric chromosome fragments during meiosis in insect spermatocytes. Mol. Biol. Cell *12*, 4054–4065.

LaFountain, J.R., Jr., Cole, R.W., and Rieder, C.L. (2002a). Partner telomeres during anaphase in crane-fly spermatocytes are connected by an elastic tether that exerts backward force and resists poleward motion. J. Cell Sci. *115*, 1541–1549.

LaFountain, J.R., Jr., Cole, R.W., and Rieder, C.L. (2002b). Polar ejection forces are operative in crane-fly spermatocytes, but their action is limited to the spindle periphery. Cell Motil. Cytoskelet. *51*, 16–26.

Maddox, P., Dasai, A., Oegema, K., Mitchison, T.J., and Salmon, E.D. (2002). Poleward microtubule flux is a major component of spindle dynamics and anaphase A in mitotic *Drosophila* embryos. Curr. Biol. *12*, 1670–1674.

Maddox, P., Straight, A., Coughlin, P., Mitchison, T.J., and Salmon, E.D. (2003). Direct observation of microtubule dynamics at kinetochores in *Xenopus* extract spindles: implications for spindle mechanics. J. Cell Biol. *162*, 377–382.

Margolis, R.L., and Wilson, L. (1981). Microtubule treadmills—possible molecular machinery. Nature *293*, 705–711.

Mitchison, T.J. (1989). Polewards flux in the mitotic spindle: evidence from photoactivation of fluorescence. J. Cell Biol. *109*, 637–652.

Mitchison, T.J., and Salmon, E.D. (1992). Poleward kinetochore fiber movement occurs during both metaphase and anaphase A in newt lung cell mitosis. J. Cell Biol. *119*, 569–582.

Nicklas, R.B. (1997). How cells get the right chromosomes. Science *275*, 632–637.

Pickett-Heaps, J.D., and Forer, A. (2001). Pac-man does not resolve the enduring problem of anaphase chromosome movement. Protoplasma *215*, 16–20.

Rieder, C.L., and Salmon, E.D. (1994). Motile kinetochores and polar ejection forces dictate chromosome position on the vertebrate mitotic spindle. J. Cell Biol. *124*, 223–233.

Rieder, C.L., and Salmon, E.D. (1998). The vertebrate cell kinetochore and its roles during mitosis. Trends Cell Biol. *8*, 310–318.

Rodionov, V.I., and Borisy, G.G. (1997). Microtubule treadmilling in vivo. Science *275*, 215–218.

Sawin, K.E., and Mitchison, T.J. (1991). Poleward microtubule flux in mitotic spindles assembled in vitro. J. Cell Biol. *112*, 941–954.

Scarcello, L.A., Janicke, M.A., and LaFountain, J.R. (1986). Kinetochore microtubules in crane-fly spermatocytes: untreated, 2°C treated and 6°C grown spindles. Cell Motil. Cytoskelet. *6*, 428–438.

Shelden, E., and Wadsworth, P. (1992). Microinjection of biotin-tubulin into anaphase cells induces transient elongation of kinetochore microtubules and reversal of chromosome-to-pole motion. J. Cell Biol. *116*, 1409–1420.

Silverman-Gavrila, R.V., and Forer, A. (2000). Evidence that actin and myosin are involved in the poleward flux of tubulin in metaphase kinetochore microtubules of crane-fly spermatocytes. J. Cell Sci. *113*, 587–609.

Waterman-Storer, C.M., and Salmon, E.D. (1997). Actomyosin-based retrograde flow of microtubules in the lamella of migrating epithelial cells influences microtubule dynamic instability and turnover and is associated with microtubule breakage and treadmilling. J. Cell Biol. *139*, 417–434.

Waterman-Storer, C.M., and Salmon, E.D. (1998). How microtubules get fluorescent speckles. Biophys. J. *75*, 2059–2069.

Waterman-Storer, C.M., and Salmon, E.D. (1999). Fluorescent speckle microscopy of microtubules: how low can you go? FASEB J. *13*, S225–S230.

Waterman-Storer, C.M., Desai, A., Bulinski, J.C., and Salmon, E.D. (1998). Fluorescent speckle microscopy, a method to visualize the dynamics of protein assemblies in living cells. Curr. Biol. *8*, 1227–1230.

Waters, J.C., Mitchison, T.J., Rieder, C.L., and Salmon, E.D. (1996). The kinetochore microtubule minus-end disassembly associated with poleward flux produces force that can do work. Mol. Biol. Cell *7*, 1547–1558.

Wilson, P.J., Forer, A., and Leggiadro, C. (1994). Evidence that kinetochore microtubules in crane-fly spermatocytes disassemble during anaphase primarily at the poleward end. J. Cell Sci. *107*, 3015–3027.

Zhai, Y., Kronebusch, P.J., and Borisy, G.G. (1995). Kinetochore microtubule dynamics and the metaphase-anaphase transition. J. Cell Biol. *131*, 721–734.